06

# The effect of temperature on the Hugoniot elastic limit and the spall strength of a lead-bismuth alloy at the pressure of shock compression up to 2.4 GPa

© A.S. Savinykh,[1,2] G.V. Garkushin,[1,2] S.V. Razorenov[1,2]

[1]Federal Research Center for Problems of Chemical Physics and Medical Chemistry, Russian Academy of Sciences, Chernogolovka, Moscow region, Russia
[2]Joint Institute for High Temperatures, Russian Academy of Sciences, Moscow, Russia
e-mail: savas@ficp.ac.ru

*Received December 9, 2022*
*Revised January 19, 2023*
*Accepted January 23, 2023*

Measurements of the Hugoniot elastic limit and the spall strength of the eutectic alloy Bi — 56.5 mass%, Pb — 43.5 mass% were carried out at sample temperatures in the range of 20−109°C based on registration and analysis of the evolution of shock compression pulses of various amplitudes. It is shown that an increase in the temperature of the samples leads to a decrease in the Hugoniot elastic limit by 25%, and the spall strength of the alloy under study — by 30%, regardless of the strain rate. An increase in the strain rate by two orders of magnitude leads to an increase in the spall strength by about three times. Approximation power-law dependences of the decay of the elastic precursor on the thickness of the samples and the spall strength on the strain rate before fracture at normal and elevated temperatures are constructed.

**Keywords:** lead-bismuth eutectic alloy, shock waves, deformation, temperature, Hugoniot elastic limit, spall strength.

DOI: 10.21883/TP.2023.03.55809.269-22

## Introduction

Lead melts with bismuth, mainly eutectic alloy Bi — 56.5 mass%, Pb — 43.5 mass%, are used as coolants in special-purpose reactors [1,2]. Studies of the thermophysical properties of liquid metal coolants began in the 1950s [3] and continue up to the present time [4–7]. Besides, heavy metals are used as targets in high-power pulsed neutron sources based on the spallation reaction (SNS — Spallation Neutron Source) [8]. The pulsed energy release is accompanied by the excitation of compression waves and cavitation phenomena in such melts, what makes it relevant to determine the strength properties of these materials both in the solid and liquid states under pulsed shocks of submicrosecond duration. Experimental studies of the properties of materials under shock loads of microsecond duration are in most cases based on measurements and analysis of the evolution of elastoplastic shock compression waves at various temperatures [9–11]. In elastoplastic material an elastic precursor is released in compression wave is distinguished, its amplitude is proportional to the value of the yield strength, and the rate of its decay is proportional to the initial rate of plastic strain. Measurements of the compression rate in the plastic shock wave provide information on the rate dependence of the flow stress at subsequent stages of the process.

The tensile strength of solids and liquids at microsecond and submicrosecond times of loading is determined by analysis of spall phenomena occurring when a compression pulse is reflected from the free or contact surface of the sample. In this case, the value of fracture stresses during spalling is in most cases determined from the analysis of the measured profile of the free surface velocity as a function of time by the method of characteristics [12,13]. Measurements of the fracture stresses (spall strength) under these conditions at different durations of the pulsed load and different temperatures provide the information on the kinetics of fracture. The obtained experimental data on spall fracture are the basis for making models of material fracture under the action of mechanical stresses in the submicrosecond range of fracture loads. This, in turn, requires reliable experimental results and understanding of the processes of strain and fracture of materials under extreme conditions.

The aims of this paper are to measure the spall strength and Hugoniot elastic limit of the eutectic alloy Bi — 56.5 mass%, Pb — 43.5 mass% at sample temperatures in the range of 20−109°C, maximum shock compression amplitude up to 2.4 GPa and strain rates before fracture in the range $10^4-10^6\,s^{-1}$ by registering and analysis of complete wave profiles, and on the basis of the data obtained plotting of rate and temperature dependences of this alloy resistance to high-rate strain and fracture in the studied range of strain rates at room and elevated temperatures of the samples.

**Table 1.** Chemical composition of eutectic alloy Bi–Pb

| Chemical composition, % | | | | | | |
|---|---|---|---|---|---|---|
| Sn | Pb | Sb | Cu | Bi | Fe | Zn |
| 0.01 | 43.7 | 0.046 | 0.004 | Res. | 0.001 | 0.001 |

## 1. Material under study. Setting up of shock wave experiments

The initial workpieces of the eutectic alloy, consisting of bismuth (56.3 mass%) and lead (43.7 mass%), were made in a vacuum furnace under order („Tinkom" LLC) in the form of bars with a diameter of 50 mm and length 150 mm. The chemical composition of the alloy under study is given in the Table 1. The delivered material is homogeneous, does not contain visible discontinuities and large inclusions. The measured value of the longitudinal speed of sound $c_l$ was $2200 \pm 10$ m/s. The density of the alloy at 20°C is 10.660 g/cm$^3$. Melting temperature — 124°C.

Plane-parallel samples for shock-wave experiments with thickness from 0.2 to 8 mm were cut by the electroerosion method, followed by manual machining (grinding and polishing) of the surface to the reflectivity required for recording the sample velocity with a laser interferometer. Finishing of the sample surface was carried out by manual grinding on abrasive paper with different grain sizes with the addition of a water-alcohol solution.

Compression shock waves of various amplitudes were generated in the samples under study under loading with aluminum impactors with thickness of 0.1 to 4 mm at a velocity of $112 \pm 10$ to $320 \pm 10$ m/s. The impactors were accelerated using a gas gun with a caliber of 50 mm. To eliminate the impactor deflection during its acceleration in the gun barrel, the latter was mounted on a polymethyl methacrylate substrate 5 mm thick, which was glued to the end of a hollow projectile 50 mm in diameter and 100 mm long made of D16 duralumin. The impactors velocity was recorded by electrocontact sensors only in experiments at room temperature. The gun barrel and the space around the sample were evacuated before the experiment. The samples were heated before shock compression by resistive heaters made of fechral wire located at a distance of 2–2.5 mm from the sample surface. The sample heating rate was $\sim 0.05$–$0.1$°C/s. The temperature was controlled by two chromel–alumel thermocouples. The difference between the thermocouple readings did not exceed 1–2°C. In each experiment the velocity profile of the free surface of the sample $u_{fs}(t)$ was continuously recorded during its loading using a VISAR laser Doppler interferometric velocimeter with high spatial and temporal resolution [14].

## 2. Measurement results of velocity profiles of free surface

Fig. 1 shows the velocity profiles of the free surface of samples of the studied Bi–Pb alloy 2 mm thick at room and elevated to 96°C initial temperatures. The velocity of aluminum impactor varied from 112 to 320 m/s at room temperature and from 112 to 211 m/s at initial temperature of 96°C. The maximum compression stresses implemented in experiments at room temperature were 0.8–2.4 GPa, at 96°C — 0.6–1.7 GPa.

The initial compression pulse at the moment of shock had a shape close to rectangular and an amplitude corresponding to the collision velocity of a pair of materials, sample–impactor. As the shock wave passes through the sample, it evolves — shape changes in accordance with the properties of the sample material. In this case (Fig. 1), on the velocity profile of the free surface the output of an elastic compression wave with amplitude $u_{HEL}$ propagating at a velocity equal to the longitudinal speed of sound $c_l$ is recorded. After the elastic compression wave a plastic wave exits onto the free surface. In the studied range of shock compression pressures the plastic

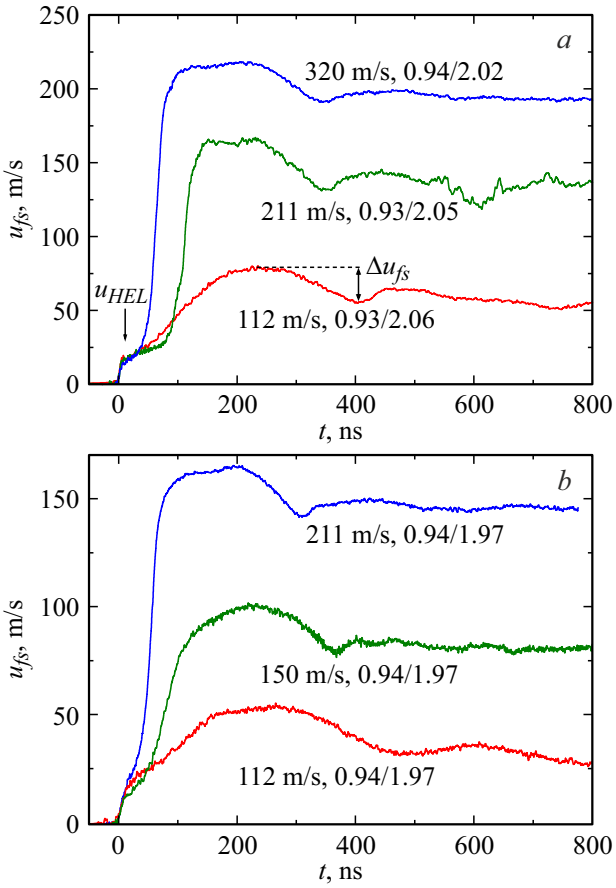


**Figure 1.** Velocity profiles of the free surface of alloy samples 2 mm thick at initial temperatures of 20 ($a$) and 96°C ($b$) and various shock velocities. The velocity of the impactor and the ratio of the thicknesses of the impactor and sample are given.

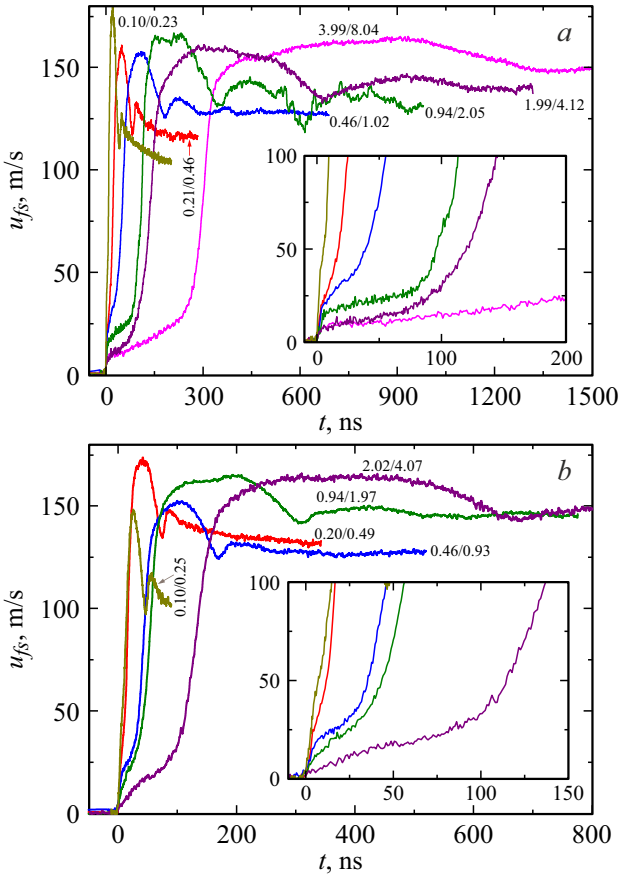


**Figure 2.** Velocity profiles of free surface of Bi–Pb eutectic alloy samples. *a* — loading of samples 0.2–8 mm thick with an aluminum impactor at speed of 211 m/s at 20°C; *b* — loading of samples 0.2–4 mm thick with aluminum impactor at velocity of 211 m/s at 96°C. The thicknesses of the impactor and sample are indicated for the profiles.

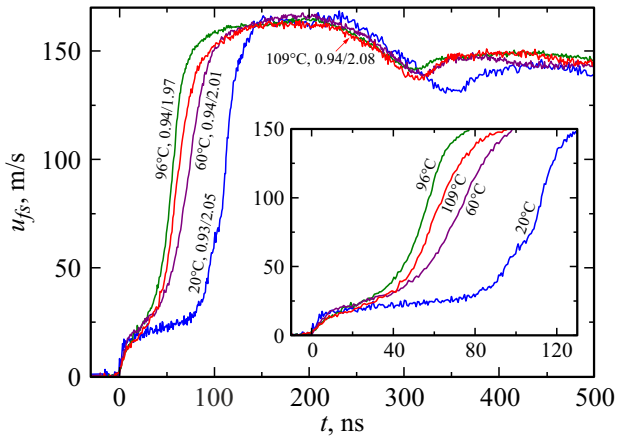


**Figure 3.** Velocity profiles of free surface of Bi–Pb eutectic alloy specimens 2 mm thick at initial temperatures of 20–109°C. Loading with aluminum striker at speed of 211 m/s. The profiles show temperature, striker and sample thicknesses.

wave has a noticeable rise time, which depends both on the shock compression pressure and on the temperature of the samples. With increase in pressure both at room temperature and at 96°C the time of velocity rise of the free surface in the plastic wave decreases significantly, besides, with increase in pressure the time between the exit of elastic and plastic waves also decreases. At initial temperature of 96°C the time between the exit of elastic and plastic waves is noticeably shorter than at room temperature. A smooth velocity increasing of the free surface between the elastic and plastic waves indicates the strain hardening of the material [11]. After the maximum surface velocity is reached, the exit of part of the rarefaction wave is recorded, which precedes the spall fracture with the amplitude $\Delta u_{fs}$, and also a weak compression pulse formed during the spall is recorded. For the eutectic alloy studied in this paper, its velocity profiles almost always show its rapid decay, and subsequent oscillations of the surface velocity associated with its reverberation in the spall plate are not recorded. No influence of the maximum compression stress on the amplitude of the elastic precursor $u_{HEL}$ and the velocity drop $\Delta u_{fs}$ in the rarefaction wave at both room temperature and 96°C was found.

Fig. 2 shows the velocity profiles of the free surface of samples 0.2–8 mm thick at room temperature and 0.2–4 mm thick at 96°C, obtained in experiments with aluminum impactor accelerated to velocity of $211 \pm 10$ m/s. The measurement results shown in Fig. 2, *a* demonstrate the decay of the elastic wave amplitude $u_{HEL}$ as it propagates in the sample, caused by the development of plastic strain and stress relaxation immediately behind its front. On the velocity profiles of the free surface of samples of different thicknesses the increase in the amplitude of the velocity drop $\Delta u_{fs}$ in the rarefaction wave with sample thickness decreasing is observed. Increasing the initial temperature of the samples to 96°C (Fig. 2, *b*) retained the same trends in the amplitude change of the elastic precursor $u_{HEL}$ and the velocity drop amplitude $\Delta u_{fs}$ with sample thickness change.

Fig. 3 shows the velocity profiles of the free surface of bismuth–lead eutectic alloy 2 mm thick at initial sample temperature of 20–109°C. The samples were loaded with aluminum impactor at velocity of $211 \pm 10$ m/s. The samples temperature increasing from 20 to 109°C led to a slight decrease in the amplitude of the elastic wave $u_{HEL}$. The velocity rise time in the elastic wave increased from 4 ns at 20°C to 10 ns at the initial temperature of 109°C. With temperature rise, the decrease in the rise time of plastic wave is recorded, which indicates decrease in the toughness of the material under study. The difference in time between the exit of elastic and plastic waves is much smaller in the experiment with sample temperature of 60°C compared to room temperature. With a further temperature increasing the time difference decreases. The larger time difference between the exit of elastic and plastic waves in the experiment at 109°C in comparison with the experiment at 96°C is due to the greater thickness of the test

sample heated to 109°C. The velocity drop amplitude in the rarefaction wave before the spall $\Delta u_{fs}$ has the largest value at room temperature and decreases with further increase in temperature.

## 3. Elastoplastic and strength properties of bismuth-lead alloy

The analysis of complete wave profiles makes it possible to obtain not only qualitative information about the nature of the response of the material under study to the action of dynamic loads of submicrosecond duration, but also to calculate its strength characteristics for these loading conditions — Hugoniot elastic limit and yield strength, critical tensile stresses during spalling, evolution kinetics of compression pulse, etc. The stress corresponding to the Hugoniot elastic limit of the material $\sigma_{HEL}$ is calculated from the amplitude of the elastic compression wave $u_{HEL}$ measured from the velocity profile of free surface $u_{fs}$ as

$$\sigma_{HEL} = \rho_0 c_l u_{HEL}/2,$$

where $c_l$ — longitudinal velocity of sound, $\rho_0$ — initial density. The values of the dynamic yield strength $\sigma_T$ under conditions of one-dimensional strain are calculated from the relation

$$\sigma_T = 3/2\sigma_{HEL}(1 - c_b^2 c_l^2),$$

where $c_b$ — volume velocity of sound.

The measured density of the bismuth–lead eutectic alloy at room temperature was 10.660 g/cm$^3$. In the paper [15] the density of the bismuth–lead eutectic alloy from 273.17 K to the melting point is described by the formula

$$\rho_0 = 10.52177 + 0.00046026T \ (273.17 < T).$$

The density dependence is shown in Fig. 4. The longitudinal velocity of sound $c_l$ measured for the alloy under study at room temperature on samples 8 mm thick was $2200 \pm 10$ m/s. In the paper [16] the change in the longitudinal velocity of sound up to temperature of 102°C was estimated, the results of this estimate are shown in Fig. 4. According to the same paper data, the bulk speed of sound $c_b$ of the bismuth–lead eutectic alloy was assumed to be 1900 m/s in the temperature range under study. The longitudinal velocity of sound at initial temperature of 109°C was calculated extrapolating the dependence shown in Fig. 4.

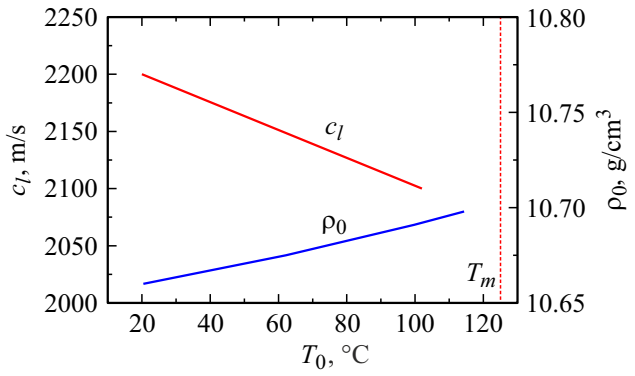


**Figure 4.** Density [15]and longitudinal velocity of sound [14] of bismuth–lead eutectic alloy vs. initial temperature. $T_m$ — alloy melting point.

After the shock wave, the rarefaction wave exits onto the surface of the sample, reducing the velocity of the free surface (Fig. 1). The first velocity minimum coincides in time with the formation of spall crack inside the sample, when tensile stresses exceeding the strength of the sample are generated by the interaction of the incident and reflected from the free surface rarefaction waves. At the moment of spall the tensile stresses relax from value equal to the critical tensile stresses (spall strength of the material) to zero, as a result a weak compression wave — a spall pulse is formed. The magnitude of the surface velocity drop $\Delta u_{fs}$ (Fig. 1) from its maximum to the first minimum before the spall pulse front is proportional to the spall strength of the material $\sigma_{sp}$. In the acoustic approximation, the value of the spall strength $\sigma_{sp}$ of the material is defined as

$$\sigma_{sp} = 1/2\rho_0 c_b(\Delta u_{fs} + \delta),$$

where $\delta$ — correction for the distortion of the velocity profile due to the difference in the velocity of the elastic front of the spall pulse equal to $c_l$, and the velocity of the plastic part of the incident rarefaction wave in front of it moving with bulk speed of sound $c_b$ [12,17].

The strain rate of the material before spall is actually the rate of expansion of the material in the rarefaction wave and is equal to

$$\frac{\dot{V}}{V_0} = -\frac{\dot{u}_{fsr}}{2c_b},$$

where $V_0$ — specific volume at zero pressure, $\dot{V}$ — volume change rate, $\dot{u}_{fsr}$ — rate of free surface velocity drop in rarefaction wave before spalling, determined from the wave profile.

Fig. 5 shows the Hugoniot elastic limit versus thickness of the sample at room and elevated to 96°C initial temperatures. The dependences shown in the Figure are obtained from experiments when samples of different thicknesses are loaded with aluminum impactor at velocity of $211 \pm 10$ m/s, which corresponds to the maximum shock compression stress $\sim 1.7$ GPa. Both at sample room temperature and at elevated temperature up to 96°C, a strong decay of the elastic wave with the distance traveled is recorded. The values of $\sigma_{HEL}$ obtained in experiments at room temperature are slightly higher than at initial temperature of 96°C over the entire measured range of sample thicknesses. It also contains data for lead grades C1 and C2, which differ from each other in the presence of impurities [18]. The measured values of $\sigma_{HEL}$ for purer lead C1 are higher than for lead C2 in the studied range of sample thicknesses. The measured values of the Hugoniot elastic limit of the studied alloy are

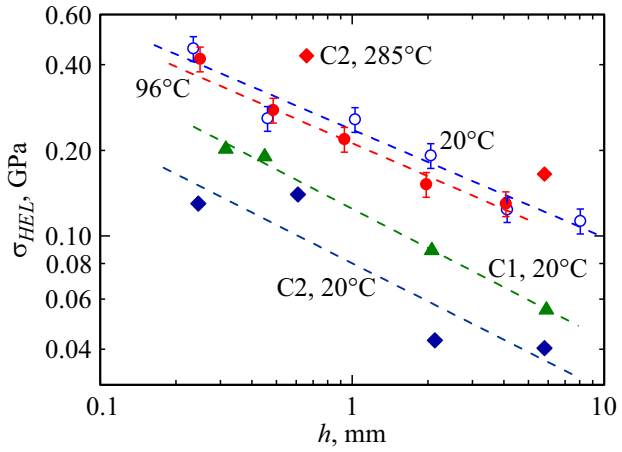


**Figure 5.** Hugoniot elastic limit vs. thickness of bismuth–lead eutectic alloy sample at room and elevated temperatures up to 96°C. Triangles — lead C1 at 20°C, dark diamonds – lead C2 at 20°C, red diamonds — lead C2 at 285°C [18].

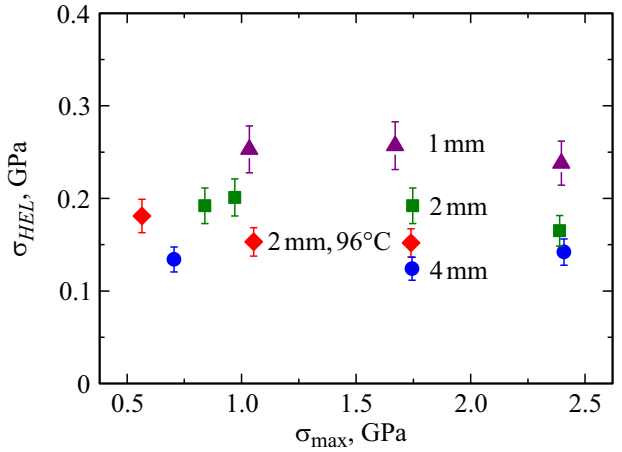


**Figure 6.** Hugoniot elastic limit vs. maximum compression stress for samples 1, 2 and 4 mm thick at room temperature and 2 mm thick at 96°C of bismuth–lead eutectic alloy.

by 2 times higher than for lead C2. Heating of lead C2 to temperatures close to its melting point results in increase in the Hugoniot elastic limit by 4 times due to the so-called athermal hardening [10], while heating of the eutectic alloy, on the contrary, slightly reduces it value.

The shown in Fig. 5 the calculated values of the Hugoniot elastic limit for the bismuth–lead eutectic alloy versus sample thickness at normal and elevated temperatures are approximated by an exponential function

$$\sigma_{HEL} = S(h/h_0)^{-\alpha}$$

where $h$ — initial sample thickness at the test temperature, $h_0 = 1$ mm, $S$ — coefficient that takes the value $\sigma_{HEL}$ at $h_0 = 1$ mm on the obtained dependence, $\alpha$ — exponent of exponential function. The use of such approximating function to describe the dependences showed that the coefficient $S$ takes the value 237 and 212 MPa for the dependences of $\sigma_{HEL}$ on the thickness of the samples for Bi–Pb eutectic alloy at room temperature and temperature increased to 96°C, respectively. The exponent $\alpha = 0.38$ — is the same both at room temperature and at 96°C. According to [18], the exponent $\alpha$ for lead C1 at room temperature and C2 at room and elevated temperatures is also the same and equals to 0.55.

Fig. 6 summarizes the data obtained for the Hugoniot elastic limit of samples of the studied alloy 1, 2 and 4 mm thick at room temperature and 2 mm thick at temperature of 96°C depending on the maximum compression stress. The elastic wave decay is observed over the entire range of realized maximum compression stresses (0.7–2.4 GPa) at room temperature. A noticeable scatter of experimental data is recorded for each thickness of the studied samples, which does not allow one to unambiguously interpret the influence of the maximum compression stress on the value of the Hugoniot elastic limit.

The results of measuring the Hugoniot elastic limit, yield strength and spall strength of samples 2 mm thick of the bismuth–lead eutectic alloy in the initial temperature range from 20 to 109°C at maximum compression stress of 1.7 GPa are shown in Fig. 7. A smooth decrease in the Hugoniot elastic limit and yield strength with increase in temperature from 20 to 109°C is ~ 25%. The drop in spall strength with temperature increasing to value close to the melting point does not exceed 30%. Fig. 7 also shows the data on the spall strength of this alloy in the liquid state at temperature of 150°C obtained in [16]. As can be seen from the Figure, the spall strength of the alloy in the liquid state is approximately by an order of magnitude lower than in the solid state at 20°C.

Spall strength of bismuth–lead eutectic alloy vs. strain rate at room and elevated temperatures up to 96°C are shown in Fig. 8. Increase in the initial temperature of the samples to 96°C, regardless of the maximum shock compression pressure, leads to decrease in the spall strength

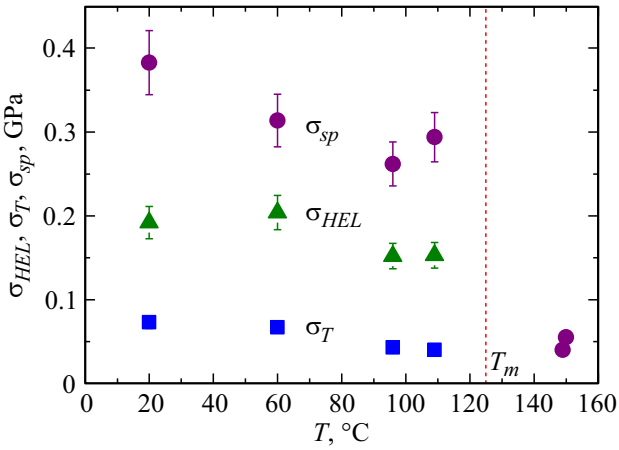


**Figure 7.** Hugoniot elastic limit, yield strength and spall strength of specimens of bismuth–lead eutectic alloy 2 mm thick vs. initial temperature. $T_m$ — alloy melting point. The spall strength values at 150°C are taken from [16].

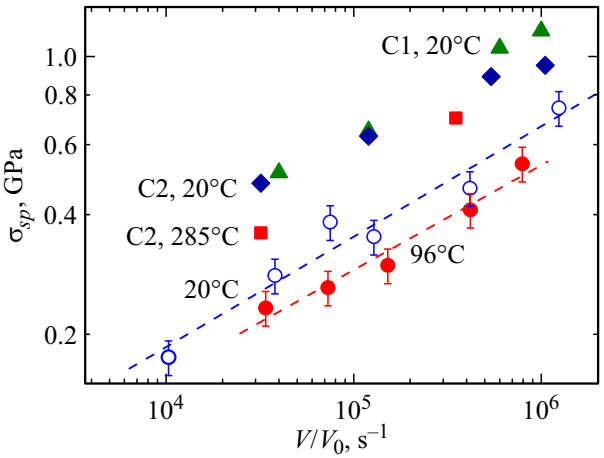


**Figure 8.** Spall strength vs. strain rate of samples of bismuth–lead eutectic alloy2 mm thick at room and elevated temperatures up to 96°C. Triangles — lead C1 at 20°C, diamonds – lead C2 at 20°C, squares — lead C2 at 285°C. Data for lead are taken from [18].

in the studied range of strain rates by about 20%. The values of spall strength of lead C1 and C2 [18] are by two times higher than the spall strength of the studied Bi–Pb alloy, and with lead temperature increasing its spall strength also decreases.

The dependences of the spall strength on the strain rate in the rarefaction wave presented in Fig. 8 can be approximated by exponential function in the form

$$\sigma_{sp} = \left(\frac{V/V_0}{\varepsilon_0}\right)^{\beta},$$

where $\varepsilon_0 = 10^5\,s^{-1}$, $A$ is the coefficient that takes the value $\sigma_{sp}$ for $\varepsilon_0 = 10^5\,s^{-1}$, $\beta$ — exponent of exponential function. At room temperature the coefficient $A$ takes the value 351 MPa, which is higher than at 96°C ($A = 290$ MPa). At room temperature the exponent is $\beta = 0.277$; as the temperature rises to 96°C, its value slightly decreases to $\beta = 0.263$. In the paper [18] the exponent $\beta$ for lead C1 and C2 at room temperature is equal to 0.225, which is somewhat lower than for bismuth–lead eutectic alloy.

## Conclusion

Experiments were performed on measuring the evolution (shaping) of wave profiles of samples of eutectic low-temperature alloy Pb–Bi (43.7/56.3) 0.2–8 mm thick at temperatures of 20, 60, 96 and 109°C in the pressure range of shock compression 0.8–2.4 GPa, its Hugoniot elastic limit and spall strength under these conditions are measured for the first time, and the following is shown. A smooth decrease in the Hugoniot elastic limit and yield strength by ~ 25% is observed with increase in samples temperature from 20 to 109°C. With increase in the strain rate by two orders of magnitude (from $\sim 10^4$ to $10^6\,s^{-1}$), the spall strength of the alloy increases by approximately three times. Increasing of the sample temperature to temperature close to the melting point results in decrease in the spall strength of the alloy by about 30%. On the basis of the obtained data, approximate exponential dependences of the decay of the elastic precursor as it propagates in the sample and the spall strength increases with increase in the strain rate before fracture at normal and elevated temperatures are plotted. The obtained results can be included in the database on the properties of reactor materials and used for predictive numerical simulation of the behavior of the studied eutectic alloy in the temperature range up to melting point under pulsed impacts.

## Funding

The work was conducted within R&D under the contract № 1770641334821000138O/226/3464-D using the equipment of the Moscow Regional Explosive Center for Collective Use of the Russian Academy of Sciences on the topic of the State Assignment № AAAA-A19-119071190040-5, the samples were prepared under the State Assignment № 075-00460-21-00.

## Conflict of interest

The authors declare that they have no conflict of interest.

## References

[1] E.O. Adamov (red.). *Mashinostroenie yadernoj tekhniki* (*Entsiklopediya „Mashinostroenie“*) (Mashinostroenie, M., 2005), tom IV-25, kn 1. (in Russian)
[2] V.I. Subbotin, M.N. Arnol'dov, F.A. Kozlov, A.L. Shimkevich. Atomic Energy, **92** (1), 29 (2002). DOI: 10.1023/A:1015050512710
[3] S.S. Kutateladze, V.M. Borishansky, I.I. Novikov, O.S. Fedynsky. *Zhidkometallicheskie teplonositeli* (Atomizdat, M., 1958) (in Russian)
[4] V.S. Chirkin. *Teplofizicheskie svojstva materialov yadernoj tekhniki. Spravochnik* (Atomizdat, M., 1968). (in Russian)
[5] K. Morita, V. Sobolev, M. Flad. J. Nucl. Mater., **362**, 227 (2007). DOI: 10.1016/j.jnucmat.2007.01.048
[6] P.S. Popel', D.A. Yagodin, A.G. Mozgovoi, M.A. Pokrasin. High Temp., **48**, 181 (2010). DOI: 10.1134/S0018151X10020070
[7] V.P. Sobolev, P. Schuurmans, G. Benamati. J. Nucl. Mater., **376**, 358 (2008). DOI: 10.1016/j.jnucmat.2008.02.030
[8] T.E. Mason, T.A. Gabriel, R.K. Crawford, K.W. Herwig, F. Klose, J.F. Ankner. *The Spallation Neutron Source: A Powerful Tool for Materials Research.* arXiv:physics/0007068 [physics.acc-ph]. DOI: 10.48550/arXiv.physics/0007068
[9] G.I. Kanel, E.B. Zaretsky, S.V. Razorenov, S.I. Ashitkov, V.E. Fortov. UFN, **187**, 525 (2017). (in Russian). DOI: 10.3367/UFNr.2016.12.038004 [G.I. Kanel, E.B. Zaretsky, S.V. Razorenov, S.I. Ashitkov, V.E. Fortov. Phys. Usp., **60** (5), 490 (2017). DOI: 10.3367/UFNe.2016.12.038004]
[10] G.I. Kanel. *Shock Waves in Solid State Physics* (CRC Press, Taylor and Francis Group, Boca Raton, London, NY., 2019)

[11] G.I. Kanel, S.V. Razorenov, V.E. Fortov. *Shock-Wave Phenomena and Properties of Condensed Matter* (Springer, NY., 2004)
[12] G.I. Kanel. Int. J. Fract., **163** (1–2), 173 (2010). DOI: 10.1007/s10704-009-9438-0
[13] T. Antoun, L. Seaman, D.R. Curran, G.I. Kanel, S.V. Razorenov, A.V. Utkin. *Spall Fracture* (Springer, NY., 2003)
[14] L.M. Barker, R.E. Hollenbach. J. Appl. Phys., **43**, 4669 (1972). DOI: 10.1063/1.1660986
[15] A.A. Aleksandrov, K.A. Orlov, V.F. Ochkov. *Svojstva i protsessy rabochikh tel i materialov atomnoj energetiki*(Izdat. dom MEI, M., 2012) (in Russian)
[16] G.V. Garkushin, A.S. Savinykh, G.I. Kanel, S.V. Razorenov. ZhETF, **155** (2), 306 (2019). (in Russian) DOI: 10.1134/S004445101902010X [G.V. Garkushin, A.S. Savinykh, G.I. Kanel, S.V. Razorenov. J. Exp. Theor. Phys., **128** (2), 268 (2019). DOI: 10.1134/S1063776119010114]
[17] G.I. Kanel. J. Appl. Mechan. Tech. Phys., **42**, 358 (2001). DOI: 10.1023/A:1018804709273
[18] A.S. Savinykh, G.I. Kanel, G.V. Garkushin, S.V. Razorenov. J. Appl. Phys., **128**, 025902 (2020). DOI: 10.1063/5.0009812

*Translated by I.Mazurov*